Detection of Experimental Autoimmune Myocarditis in Rats by ^{111}In Monoclonal Antibody Specific for Tenascin-C

Mikio Sato, MD; Tetsuya Toyozaki, MD; Kenichi Odaka, MD; Tomoya Uehara, MS; Yasushi Arano, PhD; Hiroshi Hasegawa, MD; Katsuya Yoshida, MD; Kyoko Imanaka-Yoshida, MD; Toshimichi Yoshida, MD; Michiaki Hiroe, MD; Hiroyuki Tadokoro, MD; Toshiaki Irie, PhD; Shuji Tanada, MD; Issei Komuro, MD

Background—Although the identification of inflammatory infiltrates in endomyocardial biopsy specimens is necessary for the definite diagnosis of myocarditis, the biopsy test is invasive and is not sensitive. Therefore, a new diagnostic technique for the early and noninvasive evaluation of myocarditis has been awaited. Expression of tenascin-C (TNC), one of the oligometric extracellular glycoproteins, is induced in various pathological states, including inflammation, suggesting that TNC can be a molecular marker of myocarditis.

Methods and Results—An ^{111}In anti-TNC monoclonal antibody Fab′ fragment was injected intravenously into rats with experimental autoimmune myocarditis (EAM), and the biodistribution of this radiotracer was measured. Rapid clearance of radioactivity from the blood was observed in both EAM and control rats (<1% at 6 hours after injection). Myocardial uptake of the tracer was much higher in EAM rats than in control rats (7.54-, 4.39-, and 3.51-fold at 6, 24, and 48 hours after injection, respectively). By autoradiography, high radioactivities were clearly observed in the regions indicative of inflammation in EAM rats. Single-photon emission CT imaging demonstrated the focal myocardial uptake of ^{111}In anti-TNC Fab′ in vivo.

Conclusions—Radiolabeled anti-TNC Fab′ may be useful for the noninvasive diagnosis of myocarditis. **(*Circulation*. 2002;106:1397-1402.)**

Key Words: myocarditis ■ antibodies ■ nuclear medicine

Viral infection is mostly responsible for myocarditis in humans.[1–3] The principal mechanism of heart involvement in viral myocarditis is believed to be a cell-mediated immunological reaction to cell surface changes or a new antigen related to the virus.[4] More intriguing is the possibility that viral myocarditis may culminate in dilated cardiomyopathy, presumably as a consequence of virus-mediated immunological cardiac damage.[5–7] In spite of the development of various diagnostic modalities, early and definite diagnosis of myocarditis still depends on the detection of inflammatory infiltrates in endomyocardial biopsy specimens according to the Dallas criteria.[8] However, this technique is invasive and prone to sampling error.[9] Therefore, a new diagnostic technique for the early, precise, and noninvasive diagnosis of myocarditis has been awaited.

Tenascin-C (TNC), one of the algometric extracellular matrix glycoproteins, is expressed during embryogenesis but not in normal adult tissues.[10,11] However, in various pathological states, such as wound healing, cancer invasion, or inflammation, TNC is transiently reexpressed.[12] We recently demonstrated that TNC is specifically expressed in myocardium during the active stage of myocarditis in a mouse model. Immunoreactivity of TNC appeared at the initial stage of myocytolysis, remained during the active stage while cell infiltration and necrosis continued, and disappeared with the formation of scar tissue in the healed stage.[13] This highly spatiotemporal specificity of TNC expression suggests that molecular imaging of TNC would be useful for the noninvasive diagnosis of myocarditis.

In the present study, we examined whether injected anti-TNC monoclonal antibody can target myocarditis. This antibody was used as a Fab′ fragment because of the rapid pharmacokinetics and lower immunogenicity.[14,15] Experimental autoimmune myocarditis (EAM) was induced by the immunization of rats with purified myosin with complete Freund's adjuvant.[16,17] We injected ^{111}In anti-TNC Fab′

Received March 22, 2002; revision received June 12, 2002; accepted June 12, 2002.

From the Department of Cardiovascular Science and Medicine (M.S., K.O., K.Y., I.K., H.H.), the Department of Basic Pathology (T.T), Graduate School of Medicine, and the Department of Molecular Imaging and Radiotherapy (T.U., Y.A.), Graduate School of Pharmaceutical Sciences, Chiba University, Chiba, Japan; the Department of Pathology (K.I.-Y., T.Y.), Mie University School of Medicine, Tsu, Japan; the Cardiology Division (M.H.), International Medical Center of Japan, Tokyo; and the Division of Medical Imaging (H.T., T.I., S.T.), National Institute of Radiological Sciences, Chiba, Japan.

Correspondence to Katsuya Yoshida, MD, Department of Cardiovascular Science and Medicine, Chiba University Graduate School of Medicine, 1-8-1 Inohana, Chuo-ku, Chiba-shi, Chiba 260-8670, Japan. E-mail yoshi@med.m.chiba-u.ac.jp

Circulation **is available at http://www.circulationaha.org** **DOI: 10.1161/01.CIR.0000027823.07104.86**

intravenously into EAM rats and control rats and measured its biodistribution. The localization of the radioactivity in the myocardium was also analyzed by ex vivo imaging (autoradiography) and in vivo imaging (single-photon emission CT [SPECT]).

Methods

Induction of EAM

Forty female 7-week-old Lewis rats purchased from Charles River Japan Inc (Atsugi, Kanagawa, Japan) were used under the protocol approved by the Special Committee on Animal Welfare of the Inohana Campus of Chiba University. EAM was induced in rats as previously described.[17] In brief, rats were immunized twice at a 7-day interval with 10 mg/mL porcine cardiac myosin (Sigma Chemical Co) with Freund's complete adjuvant (Sigma Chemical Co) or with Freund's complete adjuvant alone (control rats). All experiments were performed at 17 days after the first immunization.

Antibody and Western Blotting

A mouse monoclonal antibody against TNC, clone 4F10TT, was raised by immunization of a TNC-null mouse[18] with purified human TNC[19] as described previously.[13] Isolated splenic cells from a TNC-null mouse immunized with TNC were fused with SP2/0 myeloma cells. Immunoglobulin was purified from the culture supernatant of hybridoma cell clone 4F10TT cultured in serum-free media. The Fab′ fragments of the antibody were prepared by reducing the disulfide bonds of the $F(ab')_2$ fragments with mercaptoethanol after pepsin digestion of the intact antibody.

As a nonspecific control antibody, an isotype-matched monoclonal antibody against the V protein of parainfluenza virus type II (clone 53-1, isotype IgG1; kindly provided by the Department of Microbiology, Mie University School of Medicine) was also digested to the Fab′ fragment as described above.

Immunoblotting was performed as previously described.[20] In brief, hearts were removed from rats on day 21, and the myocardium was homogenized in 4 mL buffer A (20 mmol/L Tris-HCl, 0.15 mol/L NaCl, 1 mmol/L EDTA, 1 mmol/L phenylmethylsulfonyl fluoride, and 1 mmol/L dithiothreitol, pH 7.4). Samples of protein (20 μg/lane) were subjected to SDS-PAGE with 2% to 15% gradation polyacrylamide gel and electrophoretically transferred onto Immobilon membranes (Millipore). The transferred proteins were immunostained with 4F10TT (1 μg/mL) by using the indirect immunoperoxidase method.

Immunohistochemical Staining

Immunostaining of tissue sections was performed as described previously.[21] In brief, the sections were first incubated with primary antibodies 4F10TT (1 μg/mL) and then with peroxidase-conjugated anti-mouse IgG (1:500, MBL, Nagoya, Japan). After the sections were washed, diaminobenzidine/H_2O_2 solution was used to demonstrate antibody binding. The slides were lightly counterstained with hematoxylin for microscopic examination.

Radiolabeling With ^{111}In

The thiol groups of the purified Fab′ fragments of the 2 antibodies were conjugated with the maleimide groups of 1-4-[(5-maleimidopentylamino)benzyl]-EDTA (EMCS-Bz-EDTA) to place radiometal chelates distal from the antigen binding site of the antibodies, as described previously.[22,23] To a 1-mL solution of Fab′ (1 mg/mL) in 0.1 mol/L phosphate buffer (pH 6.0) was added 60 μL EMCS-Bz-EDTA (5.3 mg/mL) in the same buffer. After a 3-hour incubation, 20 μL iodoacetamide (10 mg/mL) was added to mask unreacted thiol groups. The number of EMCS-Bz-EDTA molecules conjugated per molecule of the respective antibody fragment was determined.[23] Each conjugate was then purified from unreacted low molecular weight compounds by Sephadex G-50 column chromatography (1.8 cm×40 cm), equilibrated, and eluted with MES-buffered saline (pH 6.0).

The purified conjugates were labeled with ^{111}In, as previously reported.[23] ^{111}In antibody fragments were purified by a centrifuged column procedure using Sephadex G-50 equilibrated with 0.1 mol/L PBS (pH 6.0). Radiochemical purities of the ^{111}In antibody fragments were determined by cellulose acetate electrophoresis and size-exclusion high-performance liquid chromatography.

Biodistribution Study

Ten EAM rats and 10 control rats were injected with 100 μg (111 KBq) of ^{111}In anti-TNC Fab′ in 300 μL saline solution intravenously through the tail vein. Groups of 3 or 4 animals were euthanized at 6, 24, and 48 hours after the tracer injection. Hearts, other organs (lung, liver, kidney, spleen, cerebrum, foot pad, and hindlimb muscle), and blood were weighed and then counted for radioactivity with the blood samples. Pleural effusion was also sampled in EAM rats. The percentage of the injected dose of the radioactivity per gram tissue weight was calculated. To evaluate the dose-dependent changes in EAM-targeting properties of the radiotracer, groups of 3 rats each were administered different amounts of ^{111}In anti-TNC Fab′ (10, 50, or 100 μg per rat) and euthanized at 6 hours after injection, and the uptake of the radiotracer in the heart and other organs was estimated.

The specific uptake of anti-TNC antibody in EAM rats was also estimated by comparing, at 6 hours after injection, the radioactivity distribution of the same amounts (3 μCi, 50 μg) of ^{111}In anti-TNC Fab′ (n=3) or ^{111}In nonspecific Fab′ (n=5).

Histopathologic and Quantitative Autoradiographic Study

Two groups of EAM rats were administered similar amounts (740 KBq, 50 μg) of either ^{111}In anti-TNC Fab′ or ^{111}In nonspecific Fab′. A similar amount of ^{111}In anti-TNC Fab′ was also injected into control rats. At 6 hours after injection, the hearts were excised and embedded in Tissue-Tek OCT compound (Miles). Sections of 5-μm thickness were mounted on a slide and stained with hematoxylin and eosin (H-E) for pathological analysis. Sections of 20-μm thickness were exposed to autoradiography. The imaging plate was exposed for 24 hours and studied by image analyzer (BAS-1800 system, Fuji Film Co Ltd). Autoradiographic intensities of each myocardial tissue were presented as (PSL−BG)/A, where PSL is photostimulated luminescence, BG is PSL of the background, and A is area (mm^2).

In Vivo Imaging

^{111}In anti-TNC Fab′ in vivo imaging was performed in an EAM rat by use of SPECT. The SPECT system consisted of a 3-headed γ-camera (Toshiba GCA 9300A) equipped with 1.0-mm pinhole collimators. ^{111}In anti-TNC Fab′ (2.2 MBq) was injected intravenously, and after 5.5 hours, 37 MBq of ^{99m}Tc sestamibi (MIBI) (DRL, Tokyo, Japan) was injected. Thirty minutes later, a rat was anesthetized by an intraperitoneal injection of pentobarbital (30 μg/g), and 60-minute data acquisition was performed at 120 seconds per view with stepwise rotation for each 4° over 120° and with multiple peak acquisition (15% windows for the ^{99m}Tc and both ^{111}In peaks). The matrix was 128×128 for data acquisition and for the image display with 0.6-mm pixel size.

Results

Expression of TNC in EAM Hearts

Western blot analysis of the myocardium showed that in the EAM rat, 2 strong bands were observed at ≈270 and 230 kDa (Figure 1; arrowheads, lane 2), whereas no band was observed in the normal rat myocardium (lane 1). In human glioma TNC, 3 bands were detected at ≈300, 240, and 210 kDa (arrows, lane 3).

At 21 to 28 days after the first injection of the antigen, severe inflammatory cell infiltration and myocyte necrosis were recognized throughout the myocardium (Figure 2b). Strong immunostaining for TNC was observed in the inter-

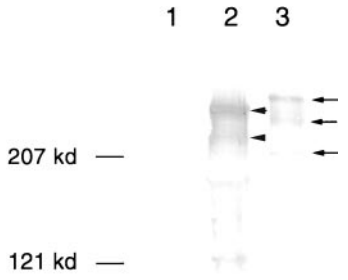

Figure 1. Western blot analysis of myocardial tissue. Extracted proteins from hearts of a normal rat (lane 1) and a rat on day 21 of myosin-induced autoimmune myocarditis (lane 2) as well as purified TNC from human glioma cells (lane 3) were electrophoresed and stained immunochemically with mouse monoclonal anti-TNC clone 4F10TT.

stitium. On the other hand, no immunostaining was detected in the normal myocardium (Figure 2a).

In Vivo Biodistribution of ^{111}In Anti-TNC Fab′

The numbers of EMCS-Bz-EDTA groups attached per antibody molecule were 1.4 and 1.6 for anti-TNC antibody and control antibody, respectively. Fewer than 0.05 free thiol groups were found per molecule of each antibody fragment after the addition of iodoacetamide. After purification by centrifuged column procedure, ^{111}In anti-TNC Fab′ and ^{111}In nonspecific Fab′ were obtained with radiochemical purities of 96.9% and 97.6% for anti-TNC antibody and the nonspecific antibody, respectively.

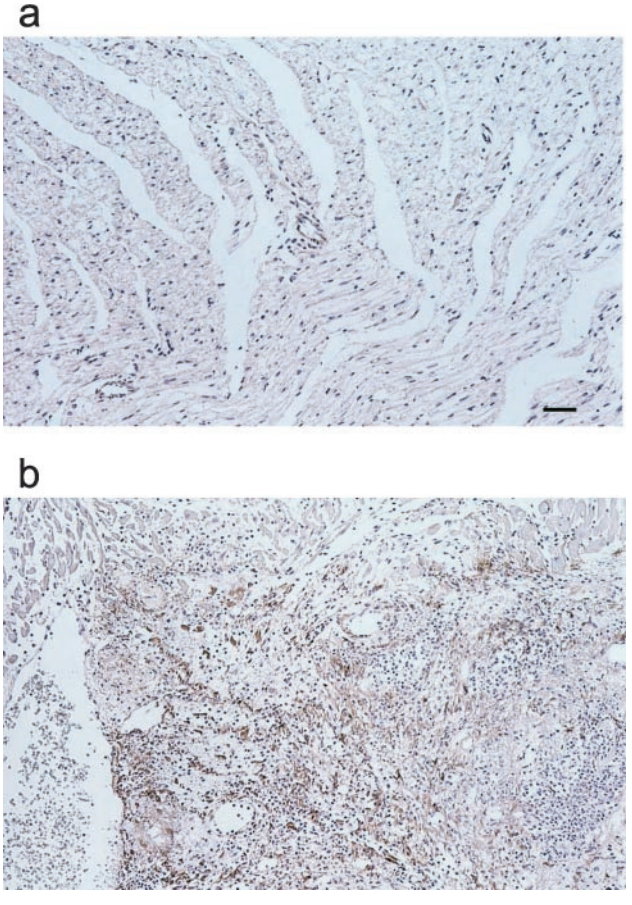

Figure 2. Immunostaining for TNC of sections from normal rat myocardial tissue (a) and from rat myocardial tissue at day 21 after first injection of myosin (b). Bar=50 μm (a).

TABLE 1. Biodistribution of ^{111}In-Labeled Anti-TNC Fab′ in EAM and Control Rats

	Time After Injection		
Tissue	6 h	24 h	48 h
EAM rats			
Blood	0.45±0.08	0.12±0.02	0.05±0.01
PE	0.44±0.06	0.29±0.04	0.12±0.03
Heart	2.39±0.17	1.06±0.13	0.59±0.20
Lung	0.76±0.08	0.48±0.06	0.48±0.17
Liver	3.05±0.26	1.70±0.33	1.20±0.27
Kidney	20.78±1.38	18.69±3.63	19.12±4.90
Spleen	6.00±0.46	5.94±1.23	4.49±1.13
Cerebrum	0.01±0.00	0.00±0.00	0.00±0.00
Foot pad	0.49±0.04	0.58±0.27	0.52±0.18
Muscle	0.15±0.17	0.09±0.04	0.05±0.01
Heart/blood	5.35±0.75	8.81±1.62	12.36±5.40
Heart/lung	3.17±0.38	2.25±0.34	1.44±0.84
Heart/liver	0.79±0.07	0.65±0.16	0.52±0.22
Control rats			
Blood	0.88±0.08	0.21±0.02	0.08±0.00
Heart	0.32±0.03	0.24±0.02	0.17±0.01
Lung	0.50±0.06	0.33±0.03	0.24±0.00
Liver	4.51±0.55	2.41±0.34	1.67±0.10
Kidney	13.34±2.36	14.75±3.34	16.78±2.89
Spleen	7.30±0.57	9.04±0.76	7.84±0.58
Cerebrum	0.02±0.00	0.01±0.00	0.00±0.00
Foot pad	0.47±0.07	1.28±0.58	0.50±0.06
Muscle	0.05±0.04	0.03±0.01	0.05±0.04
Heart/blood	0.36±0.00	1.16±0.18	2.19±0.12
Heart/lung	0.64±0.03	0.74±0.05	0.70±0.05
Heart/liver	0.07±0.00	0.10±0.01	0.10±0.01

PE indicates pulmonary effusion (nonexistent in control rats); muscle, hindlimb skeletal muscle.

Values at each time point represent mean±SD of percentage of injected dose per gram tissue weight. Each EAM or control rat received 0.3 mL ^{111}In anti-TNC Fab′ in saline (3 μCi IV).

The tissue uptake of ^{111}In anti-TNC Fab′ is summarized in Table 1 as a percentage of the injected dose per gram tissue. Rapid clearance of radioactivity from the circulation was observed with ^{111}In anti-TNC Fab′ in both EAM and control rats (<1% at 6 hours after injection). The kidney uptake was the highest at all time points, with the spleen and liver being next and then the myocardium. However, myocardial uptake was significantly lower in control rats compared with EAM rats. Radioactivity was much higher in EAM rat hearts than in control rat hearts; the increases were 7.54-, 4.39-, and 3.51-fold at 6, 24, and 48 hours, respectively. Heart-to-blood ratios of radioactivity were much higher in EAM rats than in control rats and increased gradually after injection (Table 1). Comparative myocardial uptakes with adjoining organs, such

TABLE 2. Comparison of Biodistribution Between ^{111}In Anti-TNC Fab′ and Nonspecific Fab′ in EAM Rats at 6 h After Injection

Tissue	Anti-TNC Fab′	Nonspecific Fab′
Blood	0.74±0.06	0.09±0.03
PE	0.56±0.03	0.42±0.09
Heart	2.60±0.32	0.32±0.06
Lung	0.64±0.03	0.22±0.06
Liver	6.04±0.45	0.50±0.10
Kidney	15.78±1.67	53.66±1.26
Spleen	8.53±0.42	1.00±0.12
Foot pad	0.71±0.09	0.26±0.09
Muscle	0.06±0.05	0.16±0.08

Values at each time point represent mean±SD of percentage of injected dose per gram tissue weight. Each EAM rat received 0.3 mL ^{111}In anti-TNC Fab′ or nonspecific Fab′ in saline (3 μCi IV).

as the lung and liver, are also shown in Table 1. The radiotracer reached its highest heart-to-liver and heart-to-lung ratios of radioactivity at 6 hours after injection.

The dose-dependent changes in biodistribution of ^{111}In anti-TNC Fab′ in EAM rats showed that the tracer uptake was higher with 10 μg radiolabeled antibodies in the liver and spleen than with 50 or 100 μg radiolabeled antibodies. In the heart, the tracer uptake was lower with 100 μg antibodies than with 10 or 50 μg antibodies. Thus, the antibody dose of 50 μg per rat was used in further experiments.

The comparison of radioactivity distribution between anti-TNC antibody and nonspecific antibody in EAM rats is summarized in Table 2. In the heart, much higher radioactivity was observed with an injection of ^{111}In anti-TNC Fab′ compared with an injection of ^{111}In nonspecific Fab′ (2.60±0.32 for ^{111}In anti-TNC Fab′ versus 0.32±0.06 for ^{111}In nonspecific Fab′). Radioactivity of ^{111}In anti-TNC Fab′, compared with ^{111}In-nonspecific Fab′, was lower in the kidney and higher in the blood, liver, and spleen.

Histopathologic and Quantitative Autoradiographic Study

By autoradiography, high radioactivities were observed in the region indicative of inflammation in EAM rats administered ^{111}In anti-TNC Fab′ (Figure 3, row 1). No accumulation of radioactivity was observed in EAM rats with ^{111}In nonspecific Fab′ (row 2) or in normal rats with ^{111}In anti-TNC Fab′ (row 3).

The ratios of autoradiographic intensities of each myocardial tissue in each rat group are summarized in Table 3. Because the original autoradiographic images were very small, regions of interest were placed on the autoradiograms of the whole myocardium in this analysis. High accumulation of ^{111}In anti-TNC Fab′ in EAM rat hearts was clearly shown.

In Vivo Imaging

Finally, we examined whether ^{111}In anti-TNC Fab′ imaging could be used to detect in vivo myocardial injury. SPECT imaging (Figure 4a) and autoradiography (Figure 4d) clearly showed the focal uptake of ^{111}In anti-TNC Fab′ (Figure 4a). ^{99m}Tc-MIBI myocardial perfusion imaging (Figure 4b) demonstrated the image complementary to ^{111}In anti-TNC Fab′ (Figure 4c).

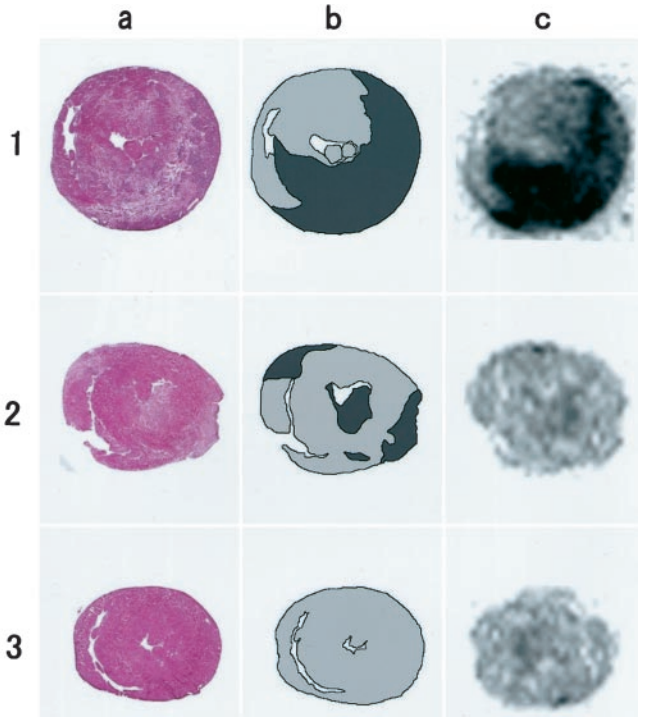

Figure 3. H-E stain (a), schema of H-E stain (b), and autoradiography (c) of adjacent sections from hearts of 3 rats (1 and 2, EAM rats; 3, normal rat) administered radiolabeled Fab′ (1, anti-TNC Fab′; 2 and 3, nonspecific Fab′). Dark-gray lesions in schema show areas of inflammatory cell infiltration and myocardial cell damage.

Discussion

Our results demonstrate that the myocardial uptake of ^{111}In anti-TNC Fab′ was significantly higher in EAM rats than in control rats. By autoradiography, high radioactivities were clearly observed in the regions indicative of inflammation in EAM rats. SPECT imaging demonstrated the suitability of this tracer for in vivo imaging.

We have recently reported that TNC was expressed at the initial stage of myocarditis in an autoimmune mouse model before necrosis or inflammatory cell infiltration was histologically apparent.[13] This result reveals the potential of early

TABLE 3. Autoradiographic Intensity Averages

	Average (PSL−BG)/A Ratio
(EAM–Anti-TNC)/(control–anti-TNC)	6.15
(EAM–anti-TNC)/(EAM–NS)	6.15
(EAM–NS)/(control–anti-TNC)	0.98

PSL indicates photostimulated luminescence; BG, PSL of background; A, area (mm^2); anti-TNC, anti-TNC antibody; and NS, nonspecific antibody.

Words in parentheses in first column show combinations of rats and monoclonal antibodies used in experiment. For example, (EAM–anti-TNC) indicates average autoradiographic intensities in EAM rat hearts injected with radiolabeled anti-TNC antibody. Regions of interest were placed on autoradiogram of whole myocardium.

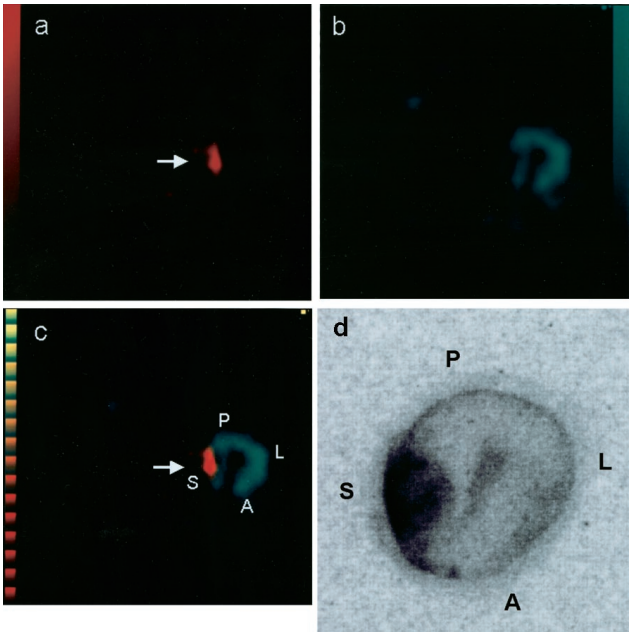

Figure 4. Transverse dual-isotope tomographic images of ^{111}In anti-TNC Fab′ and ^{99m}Tc-MIBI in EAM rat. a, Arrow shows focal uptake of ^{111}In anti-TNC Fab′. b, ^{99m}Tc-MIBI myocardial perfusion image is shown. c, Superimposed image demonstrated that focal uptake of ^{111}In anti-TNC Fab′ was detected on interventricular septum (S). d, Autoradiography. A indicates anterior; L, lateral; and P, posterior.

diagnosis of myocarditis by anti-TNC imaging. Moreover, the expression level of TNC might reflect the degree of inflammatory reactions.[13]

TNC expression is also induced in the injured cardiomyocytes in various heart diseases during the active stage.[24,25] We recently demonstrated that TNC is expressed transiently in the border zone of myocardial infarction in a rat model.[21] These data show the potential usefulness of this imaging for other forms of myocardial injury. TNC is also recognized in human coronary atherosclerotic plaque[26] or restenotic neointima after angioplasty,[27] suggesting that molecular imaging of TNC might become a useful tool for vascular injury.

^{111}In antimyosin Fab′ imaging can visualize active myocyte damage[28,29] and, thus, has been used to diagnose myocarditis.[30] ^{99m}Tc annexin-V imaging has recently been reported for the noninvasive identification of apoptotic cell death in patients with cardiac allograft rejection pathologically similar to autoimmune myocarditis.[31] Further studies are necessary to determine whether anti-TNC imaging is superior to antimyosin and annexin-V imaging.

In the present study, the anti-TNC antibody fragment was labeled with ^{111}In by using EMCS-Bz-EDTA, so that the radioactivity provides inherent in vivo behaviors of the antibody fragment.[22,32] Western blot analysis confirmed that the anti-TNC monoclonal antibody, 4F10TT, bound to 2 isoforms of rat TNC (Figure 1). Specific accumulation of 4F10TT in the inflammatory myocardium was confirmed by significantly lower accumulation of the nonspecific antibody in the hearts of EAM rats (Table 2). The regions of high accumulation of ^{111}In anti-TNC Fab′ in ex vivo imaging (autoradiography) coincided well with the regions of inflammatory cell infiltration (Figure 3), indicating that anti-TNC Fab′ is highly specific to the inflammatory region of myocarditis. This was strongly supported by SPECT imaging, in which focal uptake of ^{111}In anti-TNC Fab′ was clearly demonstrated at sites complementary to ^{99m}Tc-MIBI uptake (Figure 4). This finding also suggests that anti-TNC antibody fragments would be useful for clinical imaging, although further manipulation of the radioactivity levels in the blood, kidney, and liver is necessary.[33–35]

Although inflammation and the expression of TNC in EAM rats peak at 21 days after the first immunization,[17] all experiments were performed at 17 days because the hemodynamic abnormalities are too severe at 21 days to evaluate the kinetics of the tracer. In EAM rats, there is a characteristic initial focal inflammatory response in the myocardium, followed by massive myocardial damage at 21 days. In addition, the extent of TNC expression at 17 days is somewhat variable, as shown in Figure 3, a and b, and in Figure 4.

In conclusion, we investigated the inherent biodistribution of anti-TNC antibody Fab′ fragments in the EAM rat model. The present study indicated a high ability of the antibody fragment to localize sites of inflammation in the heart by ex vivo and in vivo imaging. Although further studies are required, radiolabeled anti-TNC fragments may be an attractive radiopharmaceutical for the noninvasive diagnosis of myocarditis.

References

1. Feldman AM, McNamara D. Myocarditis. *N Engl J Med*. 2000;343:1388–1398.
2. Hufnagel G, Pankuweit S, Richter A, et al. The European Study of Epidemiology and Treatment of Cardiac Inflammatory Diseases (ESETCID): first epidemiologic study. *Herz*. 2000;25:279–285.
3. Felker GM, Thompson RE, Hare JM, et al. Underlying causes and long-term survival in patients with initially unexplained cardiomyopathy. *N Engl J Med*. 2000;342:1077–1084.
4. Woodruff JF. Viral myocarditis: a review. *Am J Pathol*. 1980;101:427–484.
5. Kawai C. From myocarditis to cardiomyopathy: mechanisms of inflammation and cell death: learning from the past for the future. *Circulation*. 1999;99:1091–1010.
6. Abelmann WH, Lorell BH. The challenge of cardiomyopathy. *J Am Coll Cardiol*. 1989;13:1219–1239.
7. Kuhl U, Schultheiss HP. Treatment of chronic myocarditis with corticosteroids. *Eur Heart J*. 1995;16(suppl):168–172.
8. Aretz HT, Billingham M, Edwards WD, et al. Myocarditis: a histological definition and classification. *Am J Cardiovasc Pathol*. 1986;1:3–14.
9. Hauck AJ, Kearney DL, Edwards WD. Evaluation of postmortem endomyocardial biopsy specimens from 38 patients with lymphocytic myocarditis: implications for role of sampling error. *Mayo Clin Proc*. 1989;64:1235–1245.
10. Jones FS, Jones PL. The tenascin family of ECM glycoproteins: structure, function, and regulation during embryonic development and tissue remodeling. *Dev Dyn*. 2000;218:235–259.
11. Erickson HP. Tenascin-C, tenascin-R and tenascin-X: a family of talented proteins in search of functions. *Curr Opin Cell Biol*. 1993;5:869–876.
12. Chiquet-Ehrismann R, Mackie EJ, Pearson CA, et al. Tenascin interferes with fibronectin action. *Cell*. 1986;53:383–390.
13. Imanaka-Yoshida K, Hiroe M, Yasutomi Y, et al. Tenascin-C is a useful marker for disease activity in myocarditis. *J Pathol*. 2002;197:388–394.
14. Reynolds JC, Del Vecchio S, Sakahara H, et al. Anti-murine antibody response to mouse monoclonal antibodies: clinical findings and implications. *Int J Rad Appl Instrum B*. 1989;16:121–125.
15. Seccamani E, Tattanelli M, Mariani M, et al. A simple qualitative determination of human antibodies to murine immunoglobulins (HAMA) in serum samples. *Int J Rad Appl Instrum B*. 1989;16:167–170.

16. Kodama M, Zhang S, Hanawa H, et al. Immunohistochemical characterization of infiltrating mononuclear cells in the rat heart with experimental autoimmune giant cell myocarditis. *Clin Exp Immunol*. 1992;90:330–335.
17. Ishiyama S, Hiroe M, Nishikawa T, et al. The Fas/Fas ligand system is involved in the pathogenesis of autoimmune myocarditis in rats. *J Immunol*. 1998;161:4695–4701.
18. Saga Y, Yagi T, Ikawa Y, et al. Mice develop normally without tenascin. *Genes Dev*. 1992;6:1821–1831.
19. Aukhil I, Slemp CC, Lightner VA, et al. Purification of hexabrachion (tenascin) from cell culture conditioned medium, and separation from a cell adhesion factor. *Matrix*. 1990;10:98–111.
20. Kalembeyi I, Yoshida T, Iriyama K, et al. Analysis of tenascin mRNA expression in the murine mammary gland from embryogenesis to carcinogenesis: an in situ hybridization study. *Int J Dev Biol.* 1997;41:569–573.
21. Imanaka-Yoshida K, Hiroe M, Nishikawa T, et al. Tenascin-C modulates adhesion of cardiomyocytes to extracellular matrix during tissue remodeling after myocardial infarction. *Lab Invest*. 2001;81:1015–1024.
22. Arano Y, Mukai T, Akizawa H, et al. Radiolabeled metabolites of protein play a critical role in radioactivity elimination from liver. *Nucl Med Biol*. 1995;22:555–564.
23. Arano Y, Uezono T, Akizawa H, et al. Reassessment of diethylenetriaminepentaacetic acid (DTPA) as a chelating agent for indium-111 labeling of polypeptides using a newly synthesized monoreactive DTPA derivative. *J Med Chem*. 1996;39:3451–3460.
24. Tamura A, Kusachi S, Nogami K, et al. Tenascin expression in endomyocardial biopsy specimens in patients with dilated cardiomyopathy: distribution along margin of fibrotic lesions. *Heart*. 1996;75:291–294.
25. Willems IE, Arends JW, Daemen MJ. Tenascin and fibronectin expression in healing human myocardial scars. *J Pathol*. 1996;179:321–325.
26. Wallner K, Li C, Shah PK, et al. Tenascin-C is expressed in macrophage-rich human coronary atherosclerotic plaque. *Circulation*. 1999;99:1284–1289.
27. Imanaka-Yoshida K, Matsuura R, Isaka N, et al. Serial extracellular matrix changes in neointimal lesions of human coronary artery after percutaneous transluminal coronary angioplasty: clinical significance of early tenascin-C expression. *Virchows Arch*. 2001;439:185–190.
28. Khaw BA, Narula J. Antibody imaging in the evaluation of cardiovascular diseases. *J Nucl Cardiol*. 1994;1:457–476.
29. Puig M, Ballester M, Matias-Guiu X, et al. Burden of myocardial damage in cardiac allograft rejection: scintigraphic evidence of myocardial injury and histologic evidence of myocyte necrosis and apoptosis. *J Nucl Cardiol*. 2000;7:132–139.
30. Narula J, Malhotra A, Yasuda T, et al. Usefulness of antimyosin antibody imaging for the detection of active rheumatic myocarditis. *Am J Cardiol*. 1999;84:946–950.
31. Narula J, Acio ER, Narula N, et al. Annexin-V imaging for noninvasive detection of cardiac allograft rejection. *Nat Med*. 2001;12:1347–1352.
32. Arano Y, Mukai T, Uezono T, et al. A biological method to evaluate bifunctional chelating agents to label antibodies with metallic radionuclides. *J Nucl Med*. 1994;35:890–898.
33. Arano Y. Strategies to reduce renal radioactivity levels of antibody fragments. *Q J Nucl Med*. 1998;42:262–270.
34. Arano Y, Wakisaka K, Akizawa H, et al. Assessment of the radiochemical design of antibodies with a metabolizable linkage for target-selective radioactivity delivery. *Bioconjug Chem*. 1998;9:497–506.
35. Arano Y, Fujioka Y, Akizawa H, et al. Chemical design of radiolabeled antibody fragments for low renal radioactivity levels. *Cancer Res*. 1999;59:128–134.

Detection of Experimental Autoimmune Myocarditis in Rats by ^{111}In Monoclonal Antibody Specific for Tenascin-C

Mikio Sato, Tetsuya Toyozaki, Kenichi Odaka, Tomoya Uehara, Yasushi Arano, Hiroshi Hasegawa, Katsuya Yoshida, Kyoko Imanaka-Yoshida, Toshimichi Yoshida, Michiaki Hiroe, Hiroyuki Tadokoro, Toshiaki Irie, Shuji Tanada and Issei Komuro

Circulation. 2002;106:1397-1402; originally published online August 19, 2002;
doi: 10.1161/01.CIR.0000027823.07104.86
Circulation is published by the American Heart Association, 7272 Greenville Avenue, Dallas, TX 75231

Print ISSN: 0009-7322. Online ISSN: 1524-4539